Supporting Information

Multifunctional Oligomer Sponge for Efficient Solar Water Purification and Oil Cleanup

Qi Zhao, Zhongming Huang, Yingpeng Wan, Jihua Tan, Chen Cao, Shengliang Li*, and Chun-

Sing Lee*

Center of Super-Diamond and Advanced Films (COSDAF) & Department of Chemistry, City

University of Hong Kong, 83 Tat Chee Avenue, Kowloon, Hong Kong SAR, P. R. China

*Address correspondence to:

E-mail: lishengliang@iccas.ac.cn; apcslee@cityu.edu.hk

Section 1. Thermal Conductivity Measurement

Thermal conductivity of a DES sample was measured by monitoring the temperature distribution of the DES thickness between two glass slides, which is using a hot plate and ice on two sides of the foam with an IR camera (Fluke Ti400) to capture the cross-section temperature distribution. Increase the temperature of the hot plate from 60°C to 100°C in steps of 10°C. Assume that the emissivity coefficient of the glass slide and the sample is 0.9 to obtain the temperature distribution. The thermal conductivity (K) of DES is calculated using Fourier equation [33]:

$$Q' = K\, \Delta T / \Delta X$$

Assume that the thermal conductivity (K) of the glass slide is 1.05 W m^{-1} K^{-1}, then the heat flux (Q') is calculated. Since the glass slide and DES have the same heat flux, the thermal conductivity of DES is measured by using the heat flux value obtained from the glass slide.

Section 2. Energy efficiency (η) for solar steam generation

The solar-to-water evaporation efficiency (η) of DES foams can be calculated using the following formula:

$$\eta = \frac{m\, h_v}{C_{opt} P_o} \tag{1}$$

$$h_v = C\Delta T + \Delta h \tag{2}$$

where

m refers to the mass of the evaporated water under solar illumination (kg m^{-2} h^{-1}), h_v is the heat of water evaporation for the DES, C_{opt} is the optical concentration on the surface of the evaporator, and P_0 is the incident light intensity (1 kW m^{-2}). C is the specific heat capacity of water (4.18 j g^{-1} k^{-1}), ΔT is the temperature increasement of water, and Δh is the enthalpy of vaporization on the relative temperature (2250 j g^{-1}). The natural evaporation rate of water has

been subtracted from the measured solar-thermal evaporation rates by measuring the evaporation rates of water in a dark environment at the same ambient temperature and humidity. The conversion efficiency was calculated by the ratio between the harvested energy and the total solar energy. So, the solar-to-water evaporation efficiency η is calculated to be about 89%.

Section 3. Heat loss analyses

1. Conduction loss φ_1:

The conductive heat flux q_1 from DES to water is based on Fourier's law, which is calculated as follows [29-32]:

$$q_1 = K\frac{\Delta T}{X} \qquad \varphi_1 = \frac{q_1}{q}$$

where is the thermal conductivity of the DES (0.589 W m^{-1} K^{-1}) and $\Delta T/X$ is the gradient of temperature of the DES, which is approximately 43.3 K m^{-1}. q represents the emissivity, which is set to be 1 here So, the conductive loss is calculated to be 2.55%.

2. Convection energy loss φ_2:

The convection heat loss can be calculated by Newton's law of cooling:

$$q_2 = \gamma \, \Delta T \qquad \varphi_2 = \frac{q_2}{q}$$

where γ is the convection heat transfer coefficient (5 W m^{-2} K^{-1}), because of the uneven temperature distribution, here, we use average surface temperature for calculation. So, the convection energy loss is ~1.53 %.

3. Radiative energy loss φ_3:

The radiation flux can be calculated by Stefan-Boltzmann law:

$$q_3 = \varepsilon A \sigma (T_1{}^4 - T_2{}^4) \qquad \varphi_3 = \frac{q_3}{q}$$

where q_3 denotes heat flux, ε is the emissive rate, *A is the* evaporation surface surface area, σ is the Stefan-Boltzmann constant (5.67×10^{-8} W m^{-2} K $^{-4}$), T_1 is the average temperature of the absorber, and T_2 is the initial temperature in our experiment. Thus, the radiative energy loss is calculated for ~7.12 %.

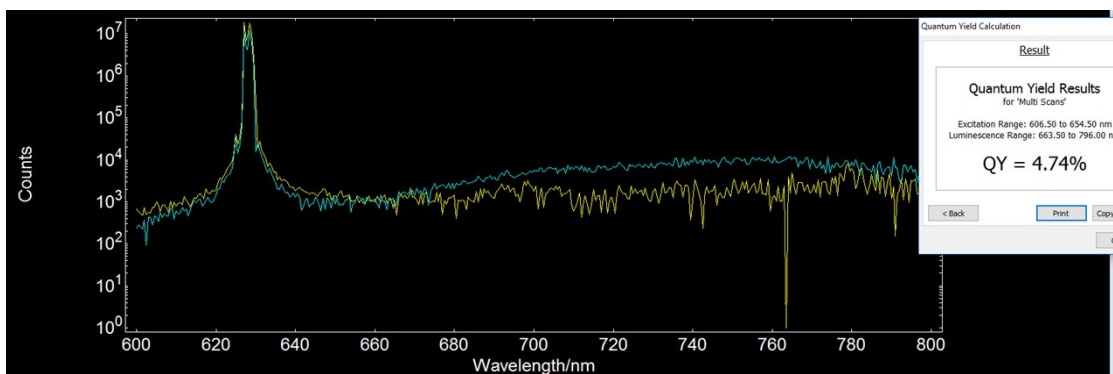**Section 4. Additional figures**
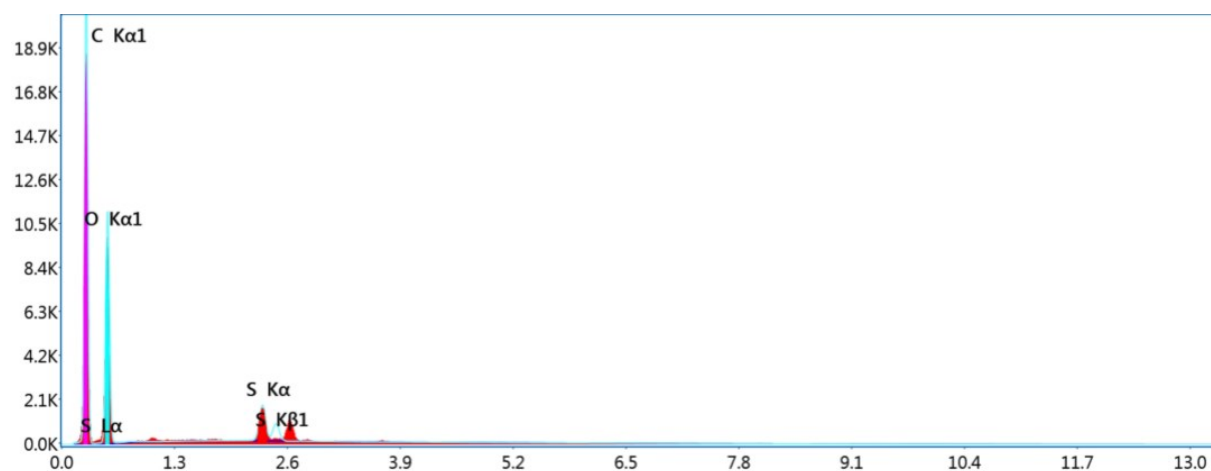
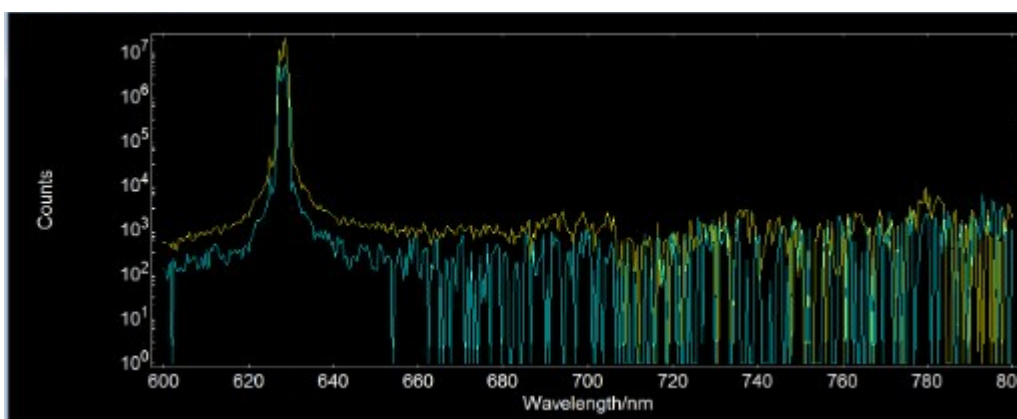**Figure S1.** EDS spectrum of DES.

A   B
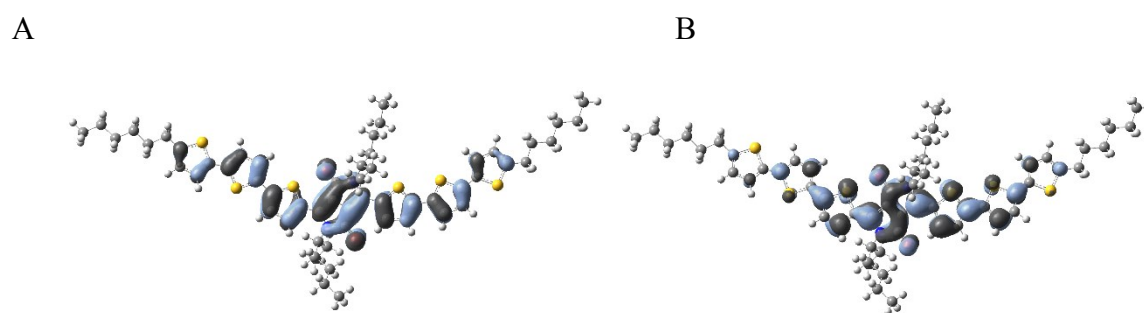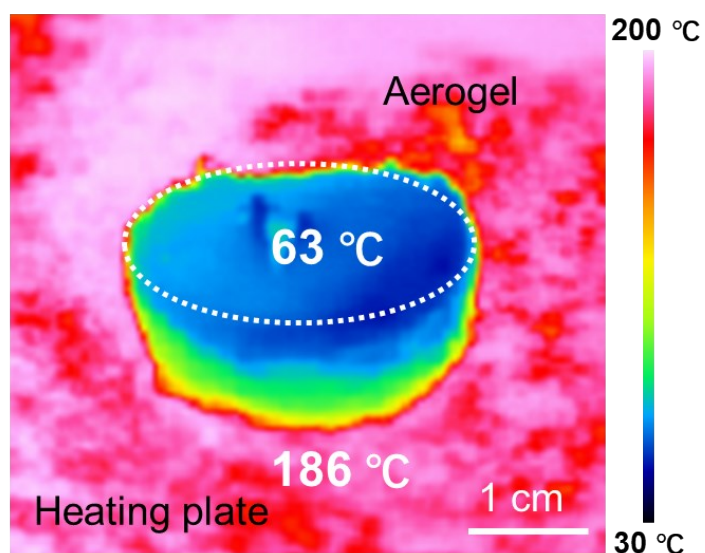

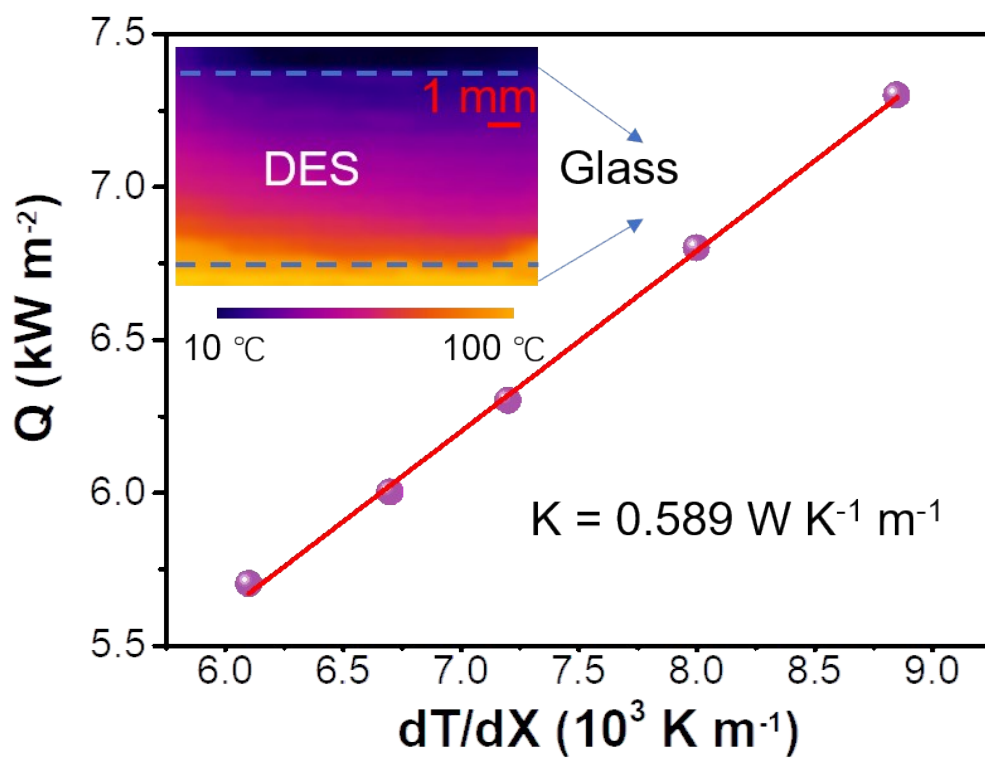**Figure S2.** The calculated HOMOs A) and LUMOs B) of the DPP-2T.

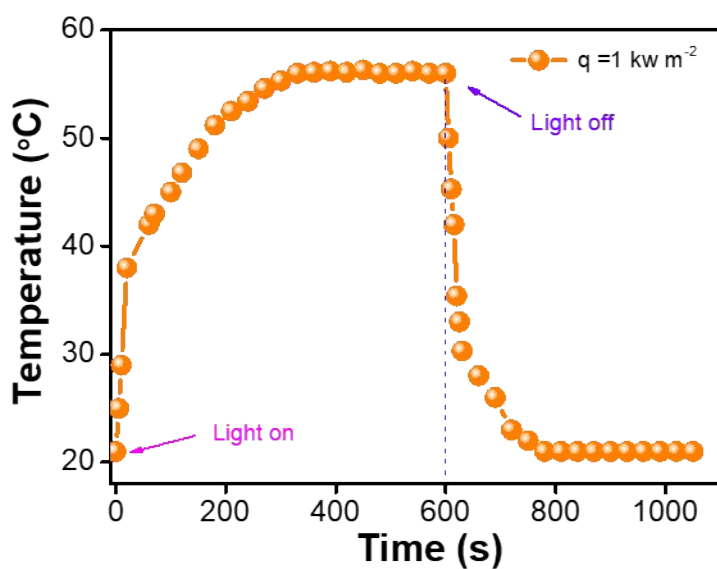**Figure S3.** PLQY of DPP-2T in THF solution.

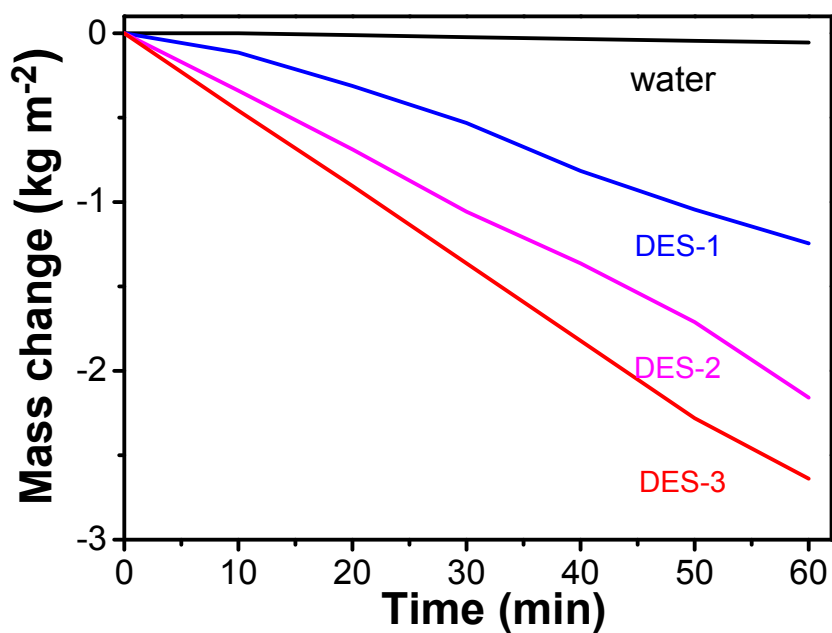**Figure S4.** PLQY of DPP-2T in the film.

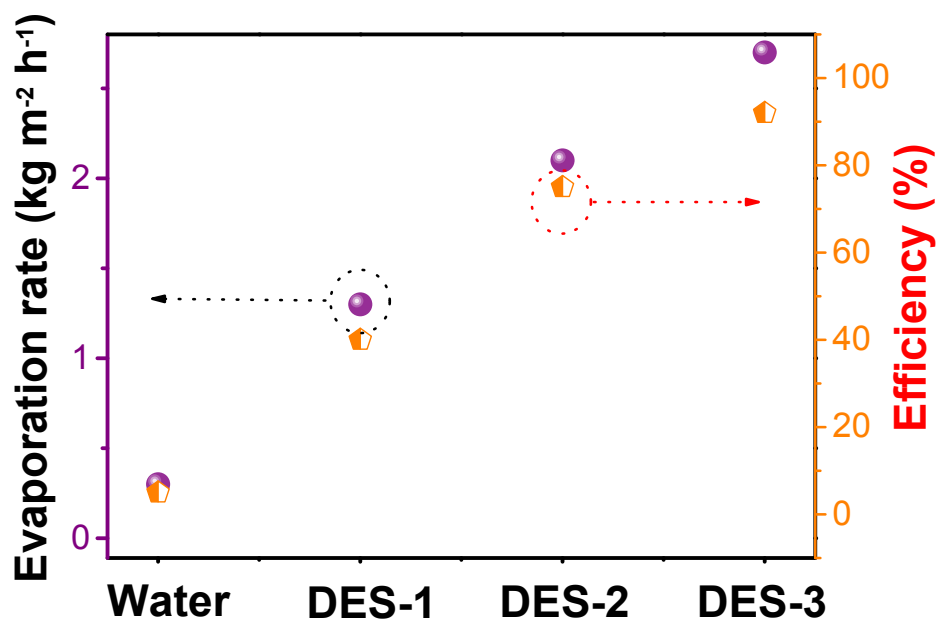**Figure S5.** Thermal insulation performance of DES.

Figure S6. Thermal conductivity of the DES. Inset is a representative IR image showing the
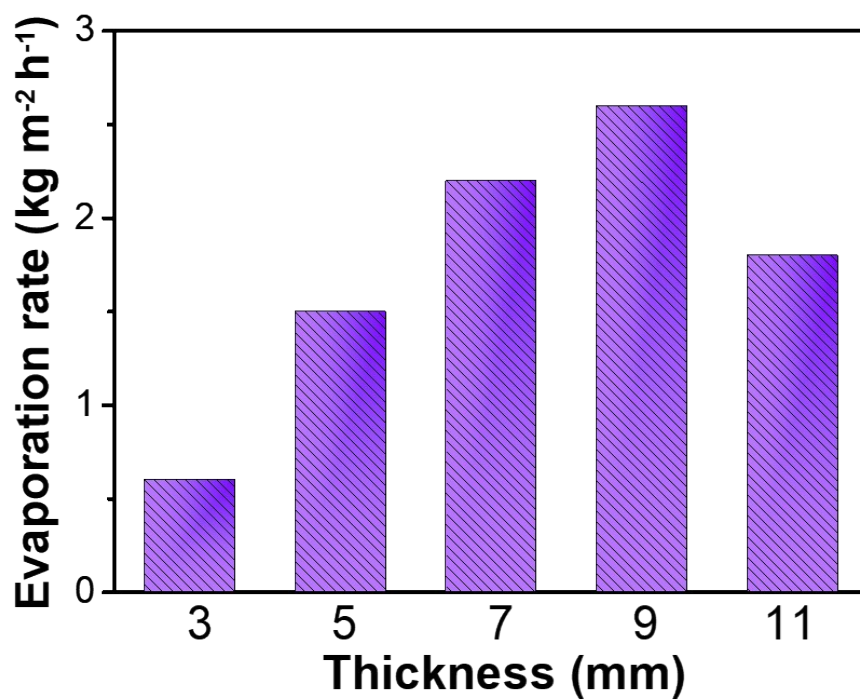
temperature gradient along the thickness of the DES.

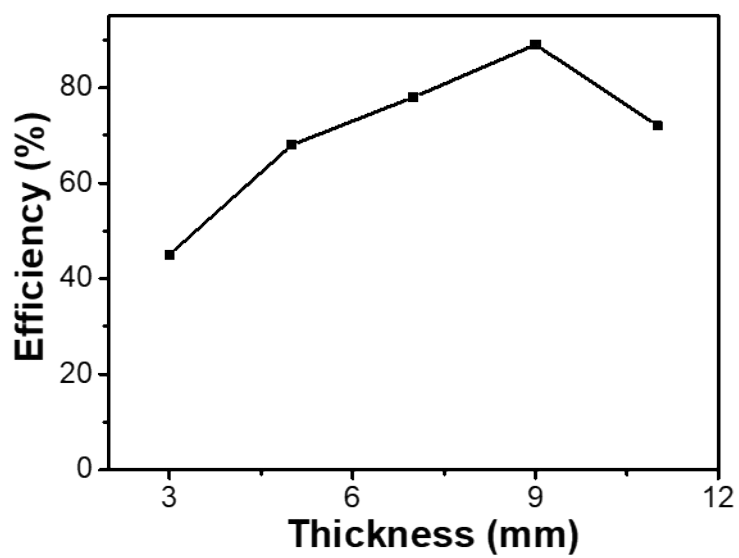**Figure S7**. Temperature changes of rGO foam under 1 Sun irradiation in air.

Figure S8. Mass changes of different DES foams under 1 sun irradiation.

Figure S9. Corresponding evaporation rates and solar-vapor efficiencies of different foams under 1 solar irradiation

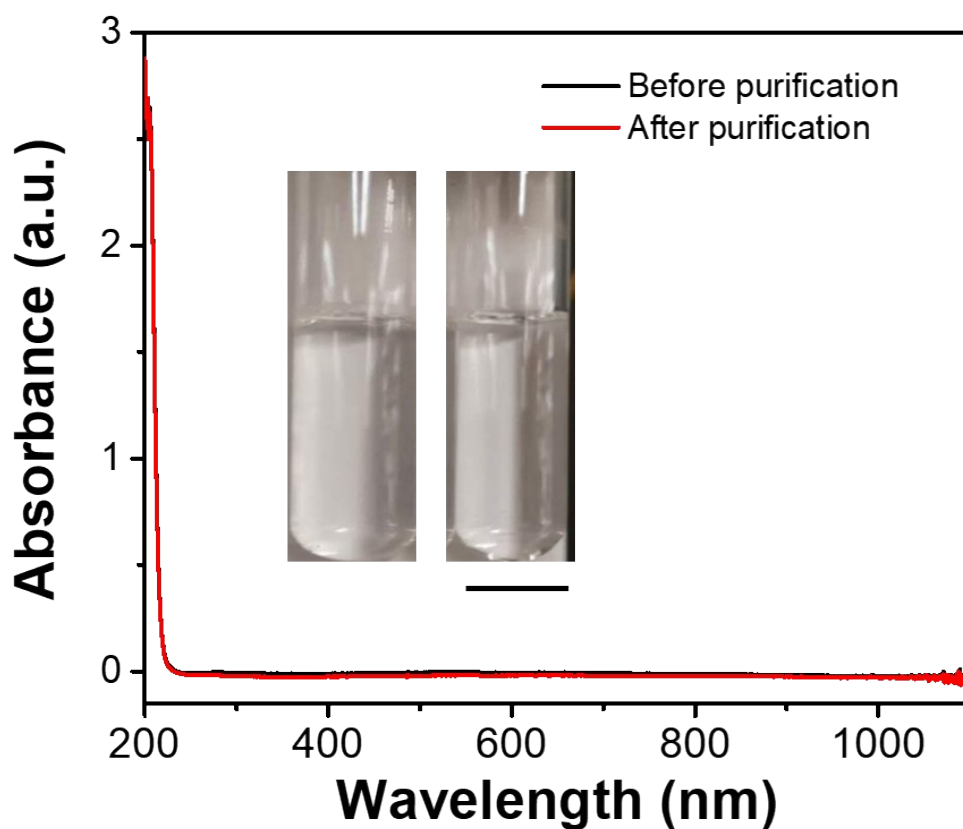**Figure S10**. Evaporation rate of DES with different thickness samples.

Figure S11. The efficiency of DES with different thickness samples.

8

Figure S12. Absorption spectra of seawater before and after desalination, scale bar: 1 cm.
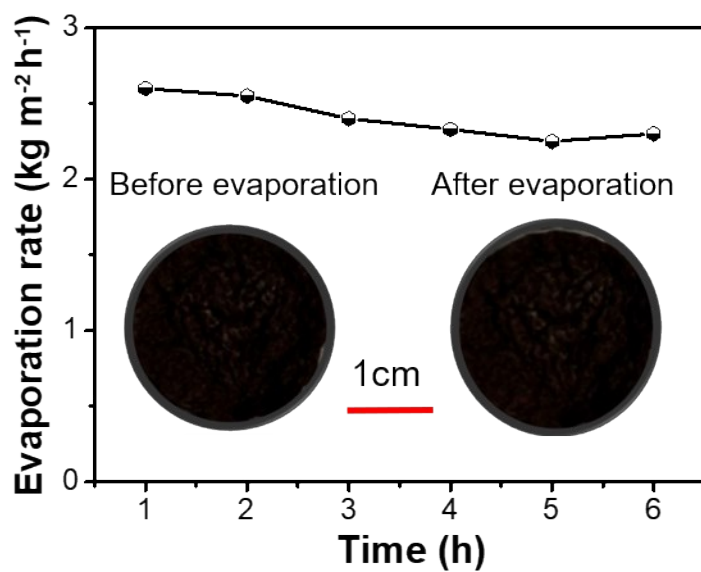
Figure S13. Long-term stability test of DES in seawater under 1 solar illumination for 6 hours. Insets are photos of DES before and after 6 hours of evaporation.
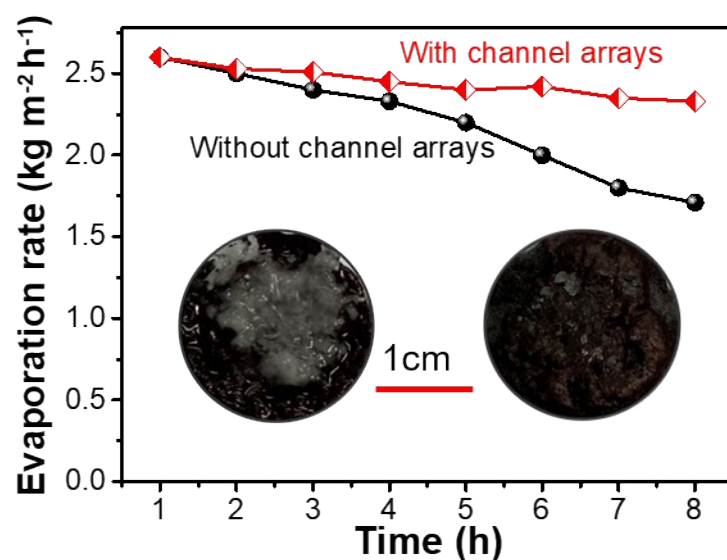
Figure S14. The evaporation rates of DES in high-salinity brine (20%) with and without an array of holes (1mm diameter) under 1 solar illumination for 8 hours. Insets are photos of DES with and without an array of holes after 8 hours of evaporation.
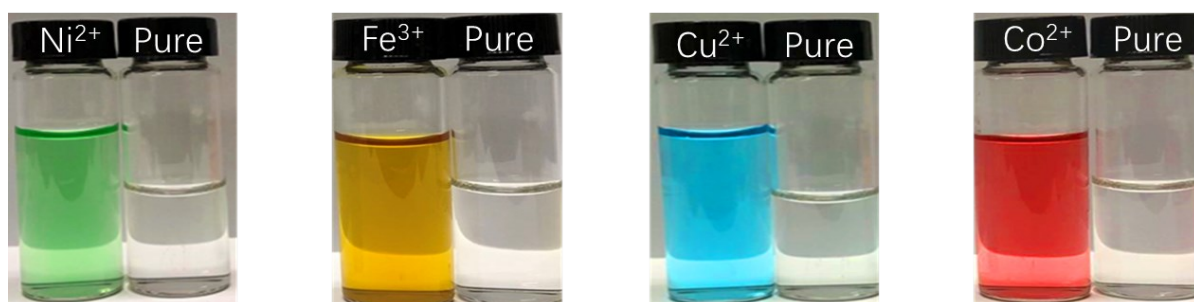
Figure S15. Photographs of wastewater samples and pure water after treatment by DES, including Ni^{2+}, Fe^{3+}, Cu^{2+}, and Co^{2+}.
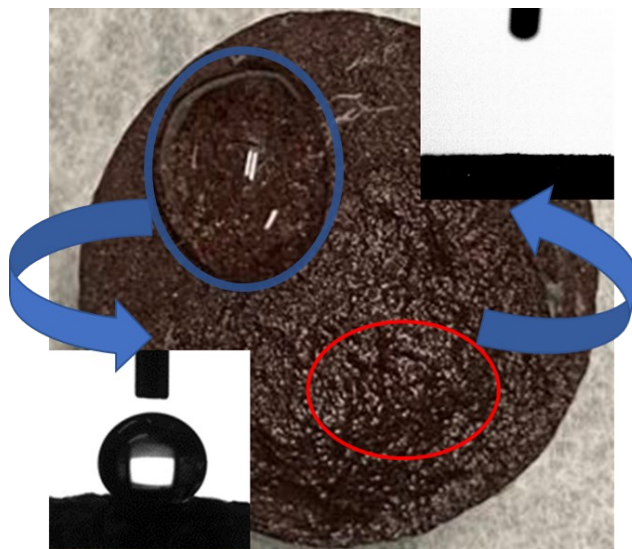
Figure S16. Optical images of the oil and water droplet profile on the surface of the DES foam and the corresponding contact angle.
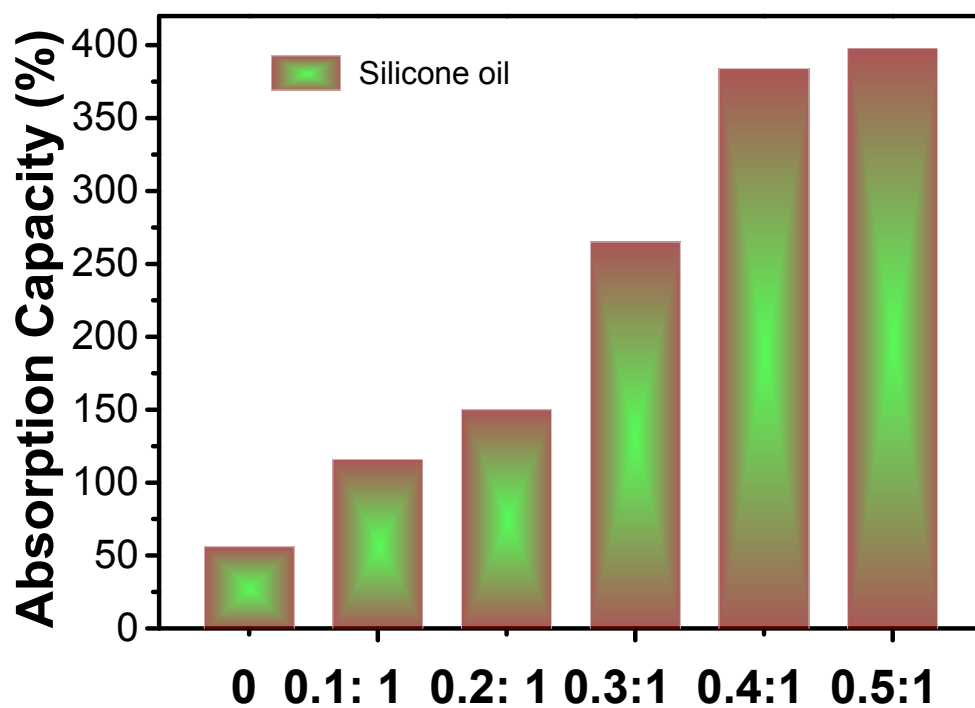
Figure S17. Silicone oil absorption capacity of DES foams with the different DPP-2T concentrations.

Figure S18. Detailed design and dimensions of the prototype.

Table S1. The solar evaporation performance of recently reported works measured under 1 sun irradiation.

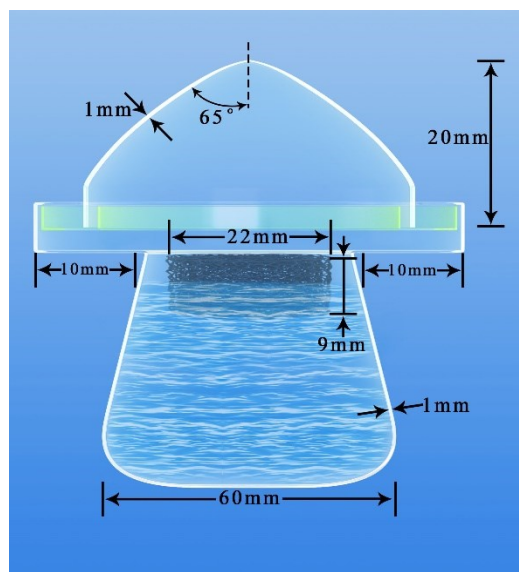| Absorber	Evaporator	m (kg m^{-2} h^{-1})	Ref.
Small molecules	DES	2.60	**This work**
	CTCC-S	1.67	(1)
	PU+CR-TPE-T	1.272	(2)
Carbon-based materials	Cabonizated wood	0.80	(3)
	PMMA / PAN / carbon black	1.3	(4)
	Carbon sponge	1.39	(5)
	3D CNT/CNC sponges	1.35	(6)
	3D cup coating with MMO pigments	1.7	(7)
	Hierarchical graphene foam	1.40	(8)
	Carbonized mushrooms	1.48	(9)
	Graphene sheets membrane	1.62	(10)
	Polyaniline-cotton fabric	1.94	(11)
	BCBF	2.8	(12)
	3D origami with CNT composite	1.59	(13)
	RHB-based sponge-like porous hydrogel	1.79	(34)
Inorganic semiconductors	Biomimetic MXene Texture	1.33	(14)
	MXene Ti$_3$C$_2$	1.32	(15)
	MOF-Based Hierarchical Structures	1.5	(16)
	MoS$_2$ hybrid film	1.1	(17)
	Ti$_2$O$_3$ nanoparticles	1.30	(18)

	3D cup-shaped solar evaporator	2.04	(19)
Plasmonic materials	Ag NP plasmonic structures	1.20	(20)
	AuFs/silica aerogel	1.36	(21)
	Bilayer SWNT/AuNR film	1.85	(22)
	Au plasmonic absorber	2.70	(23)
Polymers	PPy-coated mesh	0.92	(24)
	Polypyrrole Origamis	2.12	(25)
	PVA/PPy hierarchical gels	3.20	(26)
	PVA-PPy-Chitosan hydrogel	3.60	(27)

Section 5. References

[1]   S. Tian, Z. Huang, J. Tan, X. Cui, Y. Xiao, Y. Wan, X. Li, Q. Zhao, S. Li, C. S. Lee, *ACS Energy Lett.* **2020**, *5*, 2698.

[2]   G. Chen, J. Sun, Q. Peng, Q. Sun, G. Wang, Y. Cai, X. Gu, Z. Shuai, B. Tang, *Adv. Mater.* **2020**, *32*, 1908537.

[3]   S. He, C. Chen, Y. Kuang, R. Mi, Y. Liu, Y. Pei, W. Kong, W. Gan, H. Xie, E. Hitz, C. Jia, X. Chen, A. Gong, J. Liao, J. Li, Z. Ren, B. Yang, S. Das, L. Hu, *Energy Environ. Sci.* **2019**, *12*, 1558.

[4]   W. Xu, X. Hu, S. Zhuang, Y. Wang, X. Li, L. Zhou, S. Zhu, J. Zhu, *Adv. Energy Mater.* **2018**, *8*, 1702884.

[5]   L. Zhu, M. Gao, C. K. N. Peh, X. Wang, G. W. Ho, *Adv. Energy Mater.* **2018**, *8*,1702149.

[6]   T. Zhu, M. Ding, C. Gao, K. N. Peh, G. W. Ho, *Adv. Energy Mater.* **2019**, *9*, 1900250.

[7]   B. Zhu, G. Lv, J. Li, N. Xu, R. Lin, S. Zhu, X. Hu, X. Li, J. Zhu, G. Ni, *Natl. Sci. Rev.* **2017**, *5*, 70.

[8]   H. Ren, M. Tang, B. Guan, K. Wang, J. Yang, F. Wang, M. Wang, J. Shan, Z. Chen, D. Wei, H. Peng, Z. Liu, *Adv. Mater.* **2017**, *29*, 1702590.

[9]   N. Xu, X. Hu, W. Xu, X. Li, L. Zhou, S. Zhu, J. Zhu, *Adv. Mater.* **2017**, *29*, 1606762.

[10]   P. Zhang, J. Li, L. Lv, Y. Zhao, L. Qu, *ACS Nano* **2017**, *11*, 5087.

[11]   Z. Liu, B. Wu, B. Zhu, Z. Chen, M. Zhu, X. Liu, *Adv. Funct. Mater.* **2019**, *29*, 1905485.

[12]   Q. Zhao, Z. Huang, S. Tian, X. Cui, Y. Wan, X. Li, Y. Xiao, S. Li, C. S. Lee, *Mater. Today Energy* DOI: 10.1016/j.mtener.2020.100498.

[13]   S. Hong, Y. Shi, R. Li, C. Zhang, Y. Jin, P. Wang, *ACS Appl. Mater. Inter.* **2018**, *10*, 28517.

[14]   K. Li, T. Chang, Z. Li, H. Yang, F. Fu, T. Li, J. S. Ho, P. Y. Chen, *Adv. Energy Mater.* **2019**, *9*,

1901687

[15]   R. Li, L. Zhang, L. Shi, P. Wang, *ACS Nano* **2017**, *11*, 3752.

[16]   Q. Ma, P. Yin, M. Zhao, Z. Luo, Y. Huang, Q. He, Y. Yu, Z. Liu, Z. Hu, B. Chen, H. Zhang, *Adv. Mater.* **2019**, *31*, 1808249

[17]   X. Yang, Y. Yang, L. Fu, M. Zou, Z. Li, A. Cao, Q. Yuan, *Adv. Funct. Mater.* **2018**, *28*, 1704505.

[18]   J. Wang, Y. Li, L. Deng, N. Wei, Y. Weng, S. Dong, D. Qi, J. Qiu, X. Chen, T. Wu, *Adv. Mater.* **2017**, *29*, 1603730.

[19]   Y. Shi, R. Li, Y. Jin, S. Zhuo, L. Shi, J. Chang, S. Hong, K. C. Ng, P. Wang, *Joule* **2018**, *2*, 1171.

[20]   C. Chen, L. Zhou, J. Yu, Y. Wang, S. Nie, S. Zhu, J. Zhu, *Nano Energy* **2018**, *51*, 451.

[21]   M Gao, K. Peh, H. Phan, L. Zhu, G. W. Ho, *Adv. Energy Mater.* **2018**, *8*. 1800711.

[22]   Y. Yang, X. Yang, L. Fu, M. Zou, A. Cao, Y. Du, Q. Yuan, C. Yan, *ACS Energy Lett.* **2018**, *3*, 1165.

[23]   Z. Huang, S. Li, X. Cui, Y. Wan, Y. Xiao, S. Tian, H. Wang, X. Li, Q Zhao, C. S. Lee, *J. Mater. Chem. A.* **2020**, *8*, 10742.

[24]   L. Zhang, B. Tang, J. Wu, R. Li, P. Wang, *Adv. Mater.* **2015**, *27*, 4889.

[25]   W. Li, Z. Li, K. Bertelsmann, D. Fan, *Adv. Mater.* **2019**, *31*, 1900720.

[26]   F. Zhao, X. Zhou, Y. Shi, X. Qian, M. Alexander, X. Zhao, S. Mendez, R. Yang, L. Qu, G. Yu, *Nat. Nanotechnol.* **2018**, *13*, 489.

[28]   X. Zhou, F. Zhao, Y. Guo, B. Rosenberger, G. Yu, *Sci. Adv.* **2019**, *5*, eaaw5484.

[29]   N. Xu, X. Hu, W. Xu, X. Li, L. Zhou, S. Zhu, J. Zhu, *Adv. Mater.* **2017**, *29*, 1606762;

[30]   J. Zhou, Y. Gu, P. Liu, P. Wang, L. Miao, J. Liu, A. Wei, X. Mu, J. Li, J. Zhu, *Adv. Funct. Mater.* **2019**, *29*, 1903255.

[31]   P. Xiao, J. Gu, C. Zhang, F. Ni, Y. Liang, J. He, L. Zhang, J. Ouyang, S.-W. Kuo, T. Chen, *Nano Energy* **2019**, *65*, 104002.

[32]   X. Li, R. Lin, G. Ni, N. Xu, X. Hu, B. Zhu, G. Lv, J. Li, S. Zhu, J. Zhu, *Natl. Sci. Rev.* **2018**, *5*, 70.

[33]   H. Ghasemi, G. Ni, A. M. Marconnet, J. Loomis, S. Yerci, N. Miljkovic and G. Chen, *Nat. Commun.* **2014**, *5*, 4449.

[34]   X. Chen, Z. Wu, D. Lai, M. Zheng, L. Xu, J. Huo, Z. Chen, B. Yuan, M. Fu, *J. Mater. Chem. A* **2020**, *8*, 22645.